

WIND INTERACTION MODELS FOR THE AFTERGLOWS OF GRB 991208 and GRB 000301C

Zhi-Yun Li and Roger A. Chevalier

Department of Astronomy, University of Virginia, P.O. Box 3818

Charlottesville, VA 22903

zl4h@virginia.edu, rac5x@virginia.edu

ABSTRACT

The simplest model of the afterglows of the gamma-ray bursts (GRBs) envisions a spherical blast wave with a power-law distribution of electron energy above some cutoff running into a constant density medium. A refinement involves a narrow jet, often invoked to explain the steep decline and/or steepening of light curves observed in some afterglows. The constant (ambient) density jet model has been applied to GRBs 991208 and 000301C, based to a large extent on radio observations. We show that, for these two sources, a spherical wind model (with an r^{-2} density ambient medium) can fit the radio data as well as the jet model. The relatively steep decline and the fairly abrupt steepening of the R-band light curves of, respectively, GRB 991208 and GRB 000301C can be accounted for with a non-standard, broken power-law distribution of electron energy. Our model predicts a slower late decline for the radio flux than does the jet model.

Subject headings: gamma rays: bursts - stars: mass loss

1. INTRODUCTION

The simplest model of the afterglows of gamma-ray bursts (GRBs) involves a relativistic spherical blast wave running into a constant density, presumably interstellar, medium (Mészáros & Rees 1997; Katz 1994; see Piran 1999 for a review). The afterglows are emitted by non-thermal electrons whose energy distribution is usually assumed to be a power-law above some cutoff. The predicted power-law decay of the afterglow emission with time has been subsequently observed at X-ray (Costa et al. 1997), optical (van Paradijs et al. 1997), and radio (Frail et al. 1997) wavelengths, giving basic confirmation to this now “standard” picture.

There are observed features of afterglows that are difficult to accommodate by the simplest model. One of the most noticeable is the steepening of the optical light curves. Good examples include GRBs 990123 (Kulkarni et al. 1999), 990510 (Harrison et al. 1999; Stanek et al. 1999), and 991216 (Halpern et al. 2000). The steepening is usually attributed to a jet-like, instead of spherical, blast wave (Rhoads 1997; Sari, Piran & Halpern 1999).

Radio data are especially useful for analyzing the afterglows of GRBs because the self-absorption frequency, ν_a , and the characteristic frequency of the lowest energy electrons, ν_m , both typically lie in this range. GRB 970508 was followed extensively at radio wavelengths (Frail, Waxman, & Kulkarni 2000) and Frail et al. (2000) have suggested that there was an initial spherical relativistic expansion in a constant density medium (up to day 25), followed by lateral jet expansion (days 25–100) and spherical non-relativistic expansion (days 100–400). The same data were modeled by Chevalier & Li (2000) as a spherical blast wave running into an r^{-2} density medium characteristic of a constant mass loss rate and velocity circumstellar wind, possibly of Wolf-Rayet star origin. The model missed an early low frequency radio data point and some infrared points, but it captured most of the observed behavior over 400 days. The question of a wind vs. a constant density surrounding medium is crucial for the question of the progenitors of GRBs, because massive stars, one of the leading candidates for GRB progenitors (Paczynski 1998), should be surrounded by a wind.

Fairly extensive radio observations are now available for GRBs 991208 and 000301C (Galama et al. 2000; Berger et al. 2000). At optical wavelengths, the light curves of both sources are somewhat unusual: those of GRB 991208 are steeper than t^{-2} (Sagar et al. 2000a), and those of GRB 000301C show pronounced steepening (Rhoads & Fruchter 2000; Masetti et al. 2000; Sagar et al. 2000b; Jensen et al. 2000). These two sources have been modeled as a jet running into a constant density medium by Galama et al. (2000) and Berger et al. (2000), based on both radio and optical data. The authors ruled out the simplest, spherical wind model with a standard, power-law electron energy distribution. Here, we show that the spherical wind model fits the observed radio data as well as the constant density jet model. We also demonstrate that a non-standard distribution of electron energy can account for both the steep decline and the steepening of the optical light curves of, respectively, GRBs 991208 and 000301C. In §2, we review the spherical wind model and describe the non-standard electron energy distribution. The model is then applied to the GRBs 991208 and 000301C in §3. We discuss our results in §4.

2. WIND MODEL WITH NON-STANDARD ELECTRON ENERGY DISTRIBUTIONS

Our spherical wind interaction model was originally developed to explain the radio observations of GRB 980425/SN 1998bw (Li & Chevalier 1999), and has been subsequently applied to GRBs 980519 (Chevalier & Li 1999) and 970508 (Chevalier & Li 2000). It involves a (trans-)relativistic blast wave propagating into a circumstellar wind. Previously, we have shown that the inferred wind properties are in the range of those expected from Wolf-Rayet stars. We assume that the post-shock material is distributed uniformly inside a thin shell, and approximately determine the blast wave dynamics using shock jump conditions, and particle and energy conservation. The dynamics agree with those from the more exact self-similar solutions of Blandford & McKee (1976) to within a factor of order unity. As usual, we consider synchrotron radiation as the emission mechanism of afterglows and assume that a constant fraction ϵ_e (ϵ_B) of the total energy goes into the radiating electrons (magnetic field). The standard prescription for the energy distribution of electrons is a power-law above some minimum Lorentz factor, γ_{\min} , with a constant power-law index p . The model takes into account relativistic effects and self-absorption (important at the radio wavelengths), but not cooling. The cooling effects can be accounted for approximately once the cooling frequency ν_c is estimated (Sari, Piran & Narayan 1998; Chevalier & Li 2000). We adopt a flat universe with Hubble constant $H_0 = 65 \text{ km s}^{-1} \text{ Mpc}^{-1}$ for cosmological corrections.

The spherical wind model with the standard, power-law distribution of electron energy works rather well for GRB 970508 (Chevalier & Li 2000). Applying it to GRBs 991208 and 000301C runs into a difficulty: we cannot fit the radio and optical data simultaneously; the optical light curves do not decline with time fast enough. To overcome this difficulty, we are motivated to seek a non-standard electron energy distribution that steepens at high energies. Through trial and error, we find that a wind model with the following broken power-law distribution can fit all of the data for both sources reasonably well:

$$\frac{dN_e}{d\gamma} = C_1 \gamma^{-p_1}, \quad \text{if } \gamma_{\min} < \gamma < \gamma_b, \quad (1)$$

$$= C_2 \gamma^{-p_2}, \quad \text{if } \gamma > \gamma_b, \quad (2)$$

where γ_b is the break Lorentz factor, p_1 and p_2 are the power-law indexes for electrons below and above the break γ_b , and the coefficients C_1 and C_2 are related through $C_2 = C_1 \gamma_b^{p_2 - p_1}$ to ensure continuity of the distribution. We further assume that the ratio of the break and minimum energies, $R_b \equiv \gamma_b / \gamma_{\min}$, remains constant in time so that the relative shape of the distribution is time invariant. Given p_1 , p_2 and R_b , the minimum Lorentz factor γ_{\min} and the coefficient C_1 are determined from the total number and energy of the radiating

electrons, which in turn are determined from the dynamic evolution of the GRB blast wave. More elaborate prescriptions of the electron energy distribution may produce better fits to the observed data, but would introduce more free parameters. The implications of the above distribution on particle acceleration will be discussed in §4.

3. OBSERVED SOURCES

3.1. GRB 991208

GRB 991208 was first detected with the Interplanetary Network (IPN) by the spacecrafts *Ulysses*, WIND and NEAR on December 8, 1999, at 04:36:52 UT (Hurley et al. 2000). The main properties of its optical and radio afterglows are discussed in depth by, respectively, Sagar et al. (2000a) and Galama et al. (2000). The optical afterglow has one of the most steeply declining light curves, with the usual temporal decay index $\alpha \approx -2.2$ (Sagar et al. 2000a), assuming that the flux density evolves as $F_\nu \propto t^\alpha \nu^\beta$. The spectral index on December 16.68, 1999 is determined to be $\beta = -0.75 \pm 0.03$, based on the observed flux in the K-band (Bloom et al. 1999) and extrapolated fluxes in the R- and I-band (Sagar et al. 2000a), with negligible Galactic extinction. A day earlier on December 15.64, the fully calibrated Keck-II spectrum yields an index $\beta = -0.9 \pm 0.15$ between 3850 Å and 8850 Å (Djorgovski et al. 1999). The radio afterglow was observed extensively at a number of frequencies between 1.43 and 250 GHz over a period of two weeks (Galama et al. 2000). The multi-frequency data set allows an approximate determination by the authors of the evolution of several key synchrotron parameters: the absorption frequency $\nu_a \propto t^{-0.15 \pm 0.23}$, the “typical” frequency $\nu_m \propto t^{-1.7 \pm 0.7}$, and the peak flux density $F_m \propto t^{-0.47 \pm 0.20}$. The redshift of the source was determined to be $z = 0.706$ (Dodonov et al. 1999; Djorgovski et al. 1999).

The steep decline of the optical light curves of GRB 991208 resembles those of GRB 980326 and especially GRB 980519 (Halpern et al. 1999; Jaunsen et al. 2000). For GRB 980519, we have developed a spherical wind model with a standard power-law electron energy distribution and found that it fits the available data, from radio to optical to X-ray, reasonably well (Chevalier & Li 1999). To account for the steep light curve decline of GRB 980519 (with $\alpha = -2.05 \pm 0.04$; Halpern et al. 1999), an electron energy power-law index of about $p = 3.0$ is required. The value of p is higher than that found in other GRB afterglows (see Table 1 of Chevalier & Li 2000) but is within the range found in radio supernovae. To explain the even steeper decline of the optical light curves of GRB 991208 (with $\alpha = -2.2 \pm 0.1$; Sagar et al. 2000a) using the standard spherical wind model, an even higher value of $p \geq 3.3$ would be required (Galama et al. 2000). Such a large value

of p would be in conflict with the value $p = 2.52$ determined on December 15.5, 1999 (7.3 days after the burst) from the spectral distribution at several frequencies ranging from 1.43 GHz to R-band (Galama et al. 2000). Since the decline in the observed optical flux (with $\alpha \approx -2.2$) is much steeper than that predicted by $p = 2.52$ (which corresponds to $\alpha = -1.64$ below the cooling frequency, assuming slow cooling), the value of p should be smaller (larger) than 2.52 before (after) day 7.3 to account for the optical flux relative to that in the radio. The apparent variation required in the value of p motivates us to seek a non-standard distribution of electron energy with a non-constant power-law index p . One such non-standard distribution is the broken power-law distribution specified by equations (1) and (2) in §2.

We apply the spherical wind model with a broken power-law electron energy distribution, as described in §2, to the afterglow of GRB 991208. Through trial and error, we find that a “standard” model with the following combination of parameters fits the radio through R-band data reasonably well: the electron energy fraction $\epsilon_e = 0.03$, magnetic energy fraction $\epsilon_B = 0.01$, total blast wave energy $E = 2.7 \times 10^{52}$ ergs, wind mass loss rate $\dot{M} = 4.0 \times 10^{-6} M_\odot \text{ yr}^{-1}$ for a wind velocity of $v_w = 1,000 \text{ km s}^{-1}$, electron energy distribution power-indexes $p_1 = 2.0$ and $p_2 = 3.3$, and the ratio of the break to minimum Lorentz factors $R_b = 50$. The model fits are shown in Fig. 1. The radio data are taken from Table 1 of Galama et al. (2000) and R-band data from Table 1 of Sagar et al. (2000a). Note that the above combination of parameters is not unique. Indeed, there is a family of parameter combinations, with $\epsilon_e \propto \epsilon_B^{-1/5}$, $E \propto \epsilon_B^{-1/5}$ and $\dot{M}/v_w \propto \epsilon_B^{-2/5}$, that have the same fitting curves, as long as ϵ_B is small enough to keep the cooling frequency above the R-band at the beginning of the afterglow observations (Li & Chevalier 1999) and the electron energy distribution remains the same. Different electron energy distributions are also possible; the parameter p_2 that describes the distribution of the high energy electrons above the break is particularly ill-constrained by the light curves shown in Fig. 1 alone. It turns out that a “variant” model with a combination of the energy distribution parameters $p_1 = 2$, $p_2 = \infty$ (i.e., no high energy electrons above the break at all), and $R_b = 125$ provides an equally good fit to the radio data and a slightly better fit to the R-band data.

Additional constraints come from the spectral index β at the optical wavelengths. As mentioned earlier, a fully calibrated Keck-II spectrum yields $\beta = -0.9 \pm 0.15$ on December 15.64. At this time, the “standard” model with $p_1 = 2$, $p_2 = 3.3$, and $R_b = 50$ gives $\beta = -1.04$, within 1σ of the observed value, whereas the “variant” model with $p_1 = 2$, $p_2 = \infty$ and $R_b = 125$ gives $\beta = -1.27$, about 2σ away from the observed value. It therefore appears that p_2 should be close to 3.3. A potential difficulty is the value of $\beta = -0.75 \pm 0.03$ on December 16.68, inferred from the observed flux in the K-band (Bloom et al. 1999) and *extrapolated* fluxes in the R- and I-band (Sagar et al. 2000a). However, with only

two usable data points in the I-band (Sagar et al. 2000a) and possible deviation from a pure power-law decay in the *single* K-band measurement (Bloom et al. 1999; see R-band data for reference), we regard the index inferred on December 16.68 as less reliable than that measured simultaneously over a wide range of frequencies a day earlier. Therefore, we believe that the overall fit to both the radio and optical data is acceptable, and suspect that the fit may be improved with more elaborate prescriptions of the electron energy distribution than the simple broken power-law adopted here.

Panel (a) of Fig. 1 should be compared with Fig. 1 of Galama et al. (2000), where they fit the same radio data with a spectral form given by Granot et al. (1999a,b), based on the Blandford-McKee self-similar solution of a spherical, ultra-relativistic blast wave propagating in a constant density medium, and the best-fit power law time evolution of ν_a , ν_m , and the peak flux F_m . Inspection by eye reveals that the two model fits are of comparable quality; both models fit the three highest frequency light curves rather well. The fits to the three lowest frequency light curves are less satisfactory in *both* models, presumably because the lower frequency data are affected more by interstellar scintillation (ISS; Goodman 1997; Galama et al., in preparation). It is partially based on the low frequency data, which fix the self-absorption frequency ν_a , that Galama et al. (2000) ruled out the spherical wind model for this source. They inferred that ν_a evolves as $t^{-0.15 \pm 0.23}$, which is incompatible with the evolution, $\nu_a \propto t^{-3/5}$, predicted by a wind model. The fitted slope, -0.15 ± 0.23 , hinges, however, to a large extent on the non-detection on December 22.96 at 1.43 GHz (see the lower-right panel of their Fig. 2), the lowest observing frequency that is most affected by ISS. The poor quality of the power-law fit to the inferred values of ν_a is reflected in the relatively large reduced chi-square: $\chi_r^2 = 3.5$ for 2 degrees of freedom (see Table 3 of Galama et al. 2000). Indeed, if one were to ignore the value of ν_a based on the non-detection (the last data point in the leftmost panel of their Fig. 4), the remaining three points would yield a much steeper slope. Therefore, this piece of evidence against the wind model is not compelling in our opinion. As noted by Galama et al. (2000), the inferred evolution for two other key parameters, $\nu_m \propto t^{-1.7 \pm 0.7}$ and $F_m \propto t^{-0.47 \pm 0.20}$, is compatible with the wind model. A second objection raised by Galama et al. (2000) was that the spherical wind model requires an unusually large electron energy index, $p \geq 3.3$, to account for the steep decline of the optical light curves. This would indeed be the case if the electron energy distribution were a single power-law, as commonly assumed. The objection motivated us to seek a non-standard, broken power-law distribution of electron energy which, as demonstrated by Fig. 1, explains both the radio and R-band data reasonably well.

Based on the same set of optical and radio data, Galama et al. (2000) reached a different conclusion. They favored a constant density jet model for GRB 991208. As noted by these authors, the afterglow properties inferred from observations differ from

the *asymptotic* model predictions (Sari, Piran & Halpern 1999) on two accounts. First, the inferred decrease of the peak flux density with time, $F_m \propto t^{-0.47 \pm 0.20}$, is substantially slower than the predicted $F_m \propto t^{-1}$. Second, the inferred electron energy index $p = 2.52$ on December 15.5 is larger than the predicted $p \approx 2.2$, based on the temporal decay index of $\alpha \approx -2.2$ in R-band. The authors argued that a slow transition to the fully asymptotic regime (Kumar & Panaitescu 2000; Moderski, Sikora, & Bulik 2000) may resolve these discrepancies, since during the transition the rate of the peak flux decay *should* be between that of a spherical model, $F_m \propto t^0$, and that predicted asymptotically, $F_m \propto t^{-1}$, and the decay index α of the R-band light curve *should* be greater than $-p$ (or -2.52). While this explanation is plausible, it is far from being proven; detailed modeling of the transition is required.

The continued evolution of the radio flux provides a test of the models. Galama et al. (2000) note that in their model ν_m should pass 8.46 GHz at ~ 12 days and the flux should then decay rapidly, $F_\nu \propto t^{-2.2-2.5}$. In our model, the flux evolution at this frequency should tend to $F_\nu \propto t^{-1.25}$ (see Fig. 1). Continued monitoring of the source was apparently undertaken (Galama et al. 2000).

3.2. GRB 000301C

GRB 000301C was first detected with the RXTE All Sky Monitor and the IPN spacecrafts *Ulysses* and NEAR on March 01, 2000, at 09:51:37 UT (Smith, Hurley & Cline 2000). The IR/optical properties of its afterglow are discussed in Rhoads & Fruchter (2000), Masetti et al. (2000), Sagar et al. (2000b), and Jensen et al. (2000). Two features of the IR/optical light curves stand out: (a) large amplitude, short time scale variations and (b) a relatively abrupt steepening from a temporal decay index of $\alpha \approx -1$ to roughly -2.7 . The spectral index β was determined in the IR/optical spectral region at several times between day 2 and 14, with values ranging from ~ -0.5 to ~ -1.5 (Rhoads & Fruchter 2000; Sagar et al. 2000b; Jensen et al. 2000). The redshift of the source was determined to be 2.03 (Smette et al. 2000; Castro et al. 2000; Jensen et al. 2000). Radio light curves of varying degree of coverage are available at four frequencies (4.86, 8.46, 22.5 and 250 GHz; Berger et al. 2000), which allow for detailed modeling.

As pointed out by Berger et al. (2000), the steepening of the IR/optical light curves rules out the simplest spherical wind model *with a standard, power-law distribution of electron energy* for this source. A spherical wind model with a non-standard distribution of electron energy is still possible. Indeed, the model with a simple broken power-law distribution, outlined in §2, can fit the IR/optical light curve steepening, as well as the

radio data reasonably well. This is demonstrated in Fig. 2, where we compare the observed radio and R-band light curves with those predicted from a wind model with $\epsilon_e = 0.04$, $\epsilon_B = 0.01$, $E = 2.3 \times 10^{52}$ ergs, $\dot{M}/v_w = 4.5 \times 10^{-6} M_\odot \text{ yr}^{-1}/10^3 \text{ km s}^{-1}$, $p_1 = 2.2$, $p_2 = 15$, and $R_b = 140$. Inspection of panel (b) reveals that the model fits rather well the overall steepening of the R-band light curve, but not the short time scale variations, most noticeably the bump around day 4 and, to a lesser extent, the bump around day 7. The first bump has been interpreted by Garnavich, Loeb & Stanek (2000) as due to microlensing, although it could also be caused by a local enhancement in the ambient density (Berger et al. 2000) or an impulsive energy input (Panaitescu, Mészáros & Rees 1998; Li & Chevalier 1999; Sari & Mészáros 2000; Dai & Lu 2000). As noted by Berger et al. (2000), the physical process responsible for the first bump on the R-band light curve may also explain the factor-of-two discrepancy between the 250 GHz data taken around the same time and the model predictions (see their Fig. 2 and panel [a] of our Fig. 2). Panel (a) of Fig. 2 should be compared with Fig. 2 of Berger et al. (2000), where the same radio data set is fitted with a constant density jet model. Judging by eye, we find the quality of the two model fits comparable: the jet model fits the 250 and 22.5 GHz data slightly better, whereas the wind model fits the 8.46 and 4.86 GHz data slightly better. We note again that the combination of parameters listed above is not unique. In particular, the power-law index p_2 for the high energy electrons above the break γ_b is not well constrained. A relatively large value of p_2 is required nevertheless, to explain the rapid decline of the R-band flux at late times (with a decay index of $\alpha \approx -2.7$) in the context of the spherical wind model.

Berger et al. (2000) ruled out the possibility that the steepening in the light curves of GRB 000301C is due to a time-varying p , based on the fact that the single value, $p = 2.70$, that they inferred from a global fit to the radio/IR/optical data set, appears to fit the spectral flux distributions simultaneously at both day 4.26 and 12.17 reasonably well. Since their fitting is based on a model that assumes a *single* power-law distribution for the electron energy (i.e., a *constant* value of p at any given time), it does not necessarily rule out a curvature in the *slope* of the energy distribution (i.e., a p that *varies with energy* at any given time) as the cause for the light curve steepening. Indeed, there is some evidence for the curvature in the spectral energy distributions (SEDs) in the near IR to near UV region compiled by Rhoads & Fruchter (2000; the left panel of their Fig. 3). These SEDs are reproduced in panel (a) of our Fig. 3, with the modest amount of Galactic extinction ($E_{B-V} = 0.053$; Schlegel, Finkbeiner & Davis 1998) already corrected for. Note, however, that the data at different frequencies are not taken simultaneously and considerable uncertainties are involved in interpolating their fluxes to a common time for this source with known large amplitude, short time scale variabilities. The relatively shallow distribution at day 7.59 could, for example, be due to the previously mentioned, second (smaller) bump

on the R-band light curve around day 7, which may or may not be present in the K'-band (where the data points are too sparse to tell). Nevertheless, there appears to be a general trend that the SED steepens with time (see also column 5 of Table 3 of Rhoads & Fruchter). We expect such a steepening to occur in our model, as electrons with higher and higher energy emit into the frequency band. The spectral steepening is a robust signature of the curvature in the electron energy distribution and could in principle be used to distinguish our spherical wind model from the jet model. In panel (b) of Fig. 3, we plot the predicted SEDs of the wind model of GRB 000301C shown in Fig. 2. As expected, the SEDs steepen with time, although they are generally shallower than their observed counterparts in panel (a). A better agreement is reached if we invoke a modest amount of host galaxy extinction of $A_V = 0.09$ of the Small Magellanic Cloud (SMC) type (Pei 1992), as recommended by Rhoads & Fruchter (2000). A somewhat different value of $A_V = 0.14$, also of the SMC-type, is favored by Jensen et al. (2000) on day 3.

An alternative model for the afterglow of GRB 000301C was proposed by Kumar & Panaitescu (2000b). These authors attribute the steepening of the R-band light curve to a sudden, large drop in the density of the ambient medium into which the GRB blast wave propagates. Initially, the light curve steepens continuously as the blast wave expands freely. It tends to a constant decay rate when the observed flux is dominated by the emission from the high latitude parts of the blast wave away from the line of sight to the explosion center. This model and ours are similar in that both invoke a sudden change in either the ambient density or the electron energy distribution and that the finite light-travel time effect plays an important role in shaping the observed light curves. A potential problem with the model of Kumar & Panaitescu is that it predicts a rather steep flux decay of $t^{-2.8}$ for frequencies above ν_m but below ν_c ; the late-time decay of the observed radio flux at 8.46 GHz does not appear to be that steep (see Fig. 2), although additional observations at even later times are needed to draw a firmer conclusion.

Finally, we note that in our model even though the change in the power-law index p of the electron energy distribution is discontinuous (jumping from p_1 to p_2), the variation of the spectral index β with time is smooth (see Fig. 3b). This makes inferring the instantaneous value of p from the value of β at any given time, as has been done by, e.g., Sagar et al. (2000b), difficult.

4. DISCUSSION

Our study of these two GRBs can be separated into the radio evolution and the optical/IR evolution. ISM + jet models have been proposed for the radio emission from

both sources, but we find that spherical wind interaction models can produce fits of comparable quality. The same is true for GRB 970508 (Frail et al. 2000; Chevalier & Li 2000). In the case of GRB 991208, the approximate power law behavior observed over a factor 10 in time is intermediate between that expected for a spherical explosion in a constant density medium and the asymptotic lateral expansion of a jet (Galama et al. 2000). Kumar & Panaitescu (2000a) found that the transition to the asymptotic jet evolution should take at least an order of magnitude, perhaps several orders of magnitude, in observer time. Yet the model of Berger et al. (2000) for GRB 000301C assumes a rapid transition to the asymptotic jet evolution. The uncertainties in the jet models give them additional parameters that are not present in the wind interaction models which assume spherical symmetry throughout the evolution. Kumar & Panaitescu (2000a) found that for jet expansion in a wind medium, any break in the observed light curves would be unlikely to be detected, even for a narrow jet with an opening angle of about a few degrees. The spherical assumption, which we make, should be adequate even if a jet is present.

The problem with the simplest wind model is that the optical light curves of both GRB 991208 and GRB 000301C drop more rapidly than predicted. We have solved the problem by invoking a steepening of the electron spectrum. We attribute the steepening to the acceleration process, although the details of how this occurs are not clear. Bednarz & Ostrowski (1998) have studied acceleration in relativistic shock waves and found that at high shock Lorentz factors, the spectrum tends to a power law with $p \approx 2.2$. However, at low Lorentz factors ($\gamma \approx 3$), which are characteristic of afterglow shock waves, there are a number of possibilities, including $p < 2$, depending on the shock parameters. A particle spectrum that is this flat must steepen at high energy in order to have finite total energy. The spectral steepening with p increasing to a relatively large value of 3.3 or more that we propose for GRBs 991208 and 000301C would be clearer if X-ray observations of the sources were available. Unfortunately, these two sources are not constrained by X-ray observations. Spectral steepening with p increasing to a smaller value may also be possible. In such a case, the X-ray flux would be less affected.

The difference between an intrinsic spectral break and a laterally expanding jet is that, in the latter case, the break in a light curve should be achromatic. It appears to be difficult to decide this point solely on the basis of optical/IR observations because of the faintness of the sources and the sparse sampling. The difference between the radio and optical evolution might be clearer. The late radio light curve of GRB 000301C is most complete at 8.46 GHz and the wind model appears to give a better representation of these data than the jet model (compare Fig. [2] to Fig. [2] of Berger et al. 2000), although the uncertainties are too large to draw any firm conclusions. A similar test may be possible for GRB 991208 (see § 3.1). Another test provided by radio observations is at low frequencies. In the wind interaction

model, self-absorption is high at early times so that the low frequency flux should be low. Both GRB 970508 and GRB 000301C have one early 1.4 GHz radio observation that is higher than expected in the wind interaction model (Chevalier & Li 2000; Fig. [2]); the 1.4 GHz observations of GRB 991208 show a decrease that is not expected in any model. More extensive early, low frequency observations would provide a useful test of models.

We thank J. Rhoads for providing us with the SED data of GRB 000301C shown in Fig. 3a. This work was supported in part by NASA grant NAG5-8232.

REFERENCES

- Bednarz, J., & Ostrowski, M. 1998, *Phys. Rev. Lett.*, 80, 3911
- Berger, E., et al. 2000, *ApJ*, submitted (astro-ph/0005465)
- Blandford, R. D., & McKee, C. F. 1976, *Phys. Fluids*, 19, 1130
- Bloom, J. S., et al. 1999, GCN notice 480
- Castro, S. M., Dierks, A., Djorgovski, S. G., et al. 2000, GCN notice 605
- Chevalier, R. A., & Li, Z.-Y. 1999, *ApJ*, 520, L29
- Chevalier, R. A., & Li, Z.-Y. 2000, *ApJ*, 536, 195
- Costa, E., et al. 1997, *Nature*, 387, 783
- Dai, Z. G., & Lu, T. 2000, preprint (astro-ph/0005417)
- Djorgovski, S. G., et al. 1999, GCN notice 481
- Dodonov, S. N., Afanasiev, V. L., Sokolov, V. V., Moiseev, A. V., & Castro-Tirado, A. J. 1999, GCN notice 475
- Frail, D. A., Kulkarni, S. R., Nicastro, L., Feroci, M., & Taylor, G. B. 1997, *Nature*, 389, 261
- Frail, D. A., Berger, E. et al. 2000a, *ApJ*, 538, L129
- Frail, D. A., Waxman, E., & Kulkarni, S. R. 2000b, *ApJ*, 537, 191
- Galama, T. J., et al. 2000, *ApJ*, 541, in press (astro-ph/0006201)
- Garnavich, P. M., Loeb, A., & Stanek, K. Z. 2000, *ApJ*, submitted (astro-ph/0008049)
- Goodman, J. 1997, *New Astr.*, 2, 449
- Granot, J., Piran, T., & Sari, R. 1999a, *ApJ*, 513, 679
- Granot, J., Piran, T., & Sari, R. 1999b, *ApJ*, 527, 236
- Halpern, J. P., Kemp, J., Piran, T., & Bershadsky, M. A. 1999, *ApJ*, 517, L105
- Halpern, J. P., et al. 2000, *ApJ*, in press (astro-ph/0006206)
- Harrison, F. A., et al. 1999, *ApJ*, 523, L121

- Hurley, et al. 2000, ApJ, 534, L23
- Jaunsen, A. O. 2000, ApJ, in press (astro-ph/0007320)
- Jensen, B. L., et al. 2000, A&A, submitted (astro-ph/0005609)
- Katz, J. I. 1994, ApJ, 432, L107
- Kulkarni, S. R., et al. 1999, Nature, 398, 389
- Kumar, P., & Panaitescu A. 2000a, ApJ, 541, L9
- Kumar, P., & Panaitescu A. 2000b, ApJ, submitted (astro-ph/0006317)
- Li, Z.-Y., & Chevalier, R. A. 1999, ApJ, 526, 716
- Masetti, N., et al. 2000, A&A, 359, L23
- Mészáros, P. & Rees, M. J. 1997, ApJ, 476, 232
- Moderski, R., Sikora, M., & Bulik, T. 2000, ApJ, 529, 151
- Paczynski, B. 1998, ApJ, 494, L45
- Panaitescu, A., Mészáros, P., & Rees, M. J. 1998, ApJ, 503, 315
- Pei, Y. C. 1992, ApJ, 395, 130
- Piran, T. 1999, Phys. Rep., 314, 575
- Rhoads, J. E. 1997, ApJ, 487, L1
- Rhoads, J. E., & Fruchter, A. S. 2000, ApJ, submitted (astro-ph/0004057)
- Sagar, R., Mohan, V., Pandey, A. K., Pandey, S. B., & Castro-Tirado, A. J. 2000a, Bull. Astr. Soc. India, 28, 15
- Sagar, R., Mohan, V., Pandey, S. B., Pandey, A. K., Stalin, C. S., & Castro-Tirado, A. J. 2000b, Bull. Astr. Soc. India, in press (astro-ph/0004223)
- Sari, R., & Mészáros, P. 2000, preprint (astro-ph/0003406)
- Sari, R., Piran, T., & Halpern, J. P. 1999, ApJ, 519, L17
- Sari, R., Piran, T., & Narayan, R. 1998, ApJ, 497, L17
- Schlegel, D. J., Finkbeiner, D. P., & Davis, M. 1998, ApJ, 500, 525

Smette, A., et al. 2000, ApJ, submitted (astro-ph/0007202)

Smith, D. A., Hurley, K., & Cline, T. 2000, GCN notice 568

Stanek, K. Z., Garnavich, P. M., Kaluzny, J., Pych, W., & Thompson, I. 1999, ApJ, 522,
L39

van Paradijs, J., et al. 1997, Nature, 386, 686

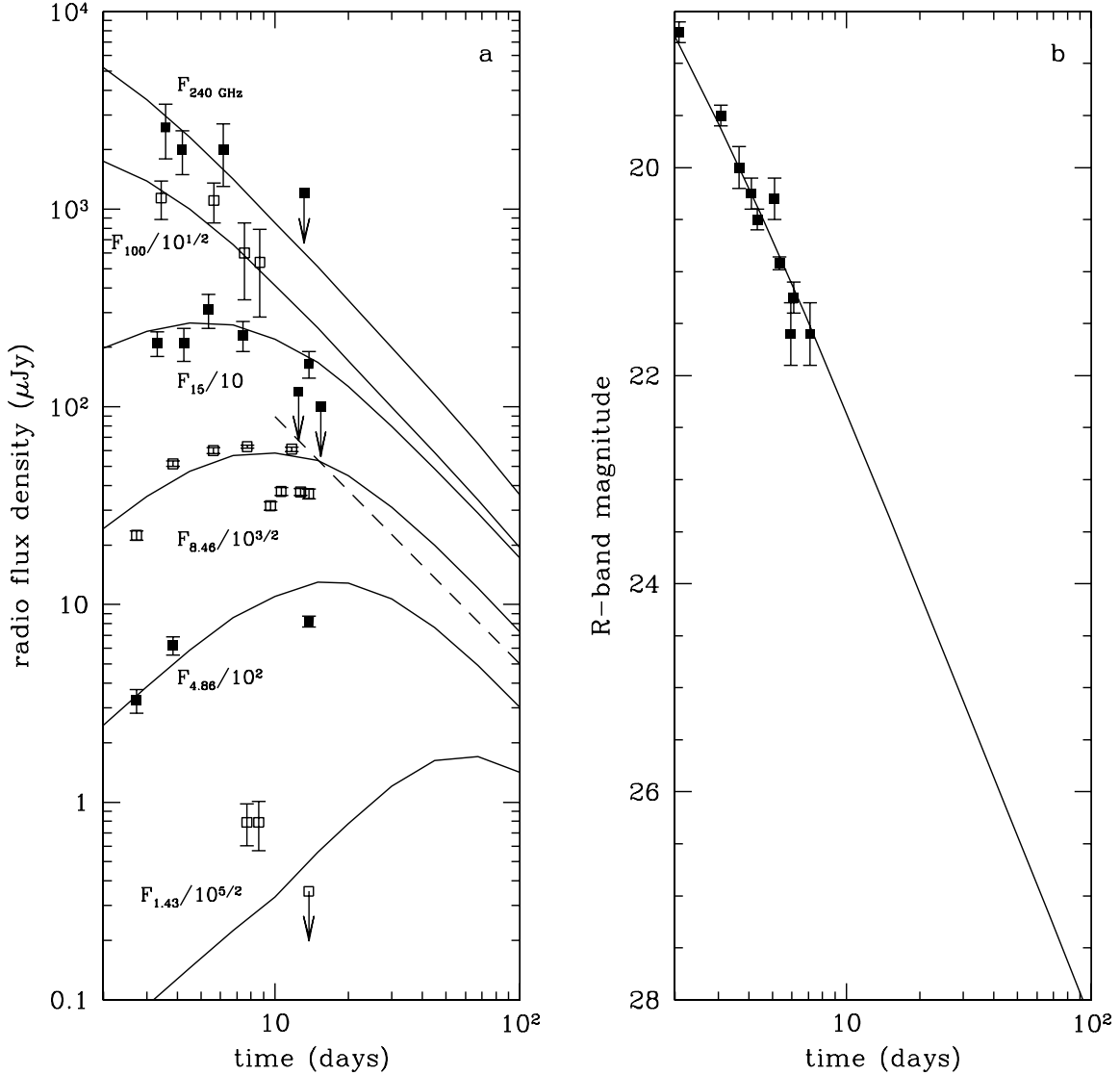


Fig. 1.— The fits of a spherical wind model with a broken power-law electron energy distribution to the observed (a) radio and (b) R-band data of GRB 991208. The model is described in §2 and the model parameters in §3.1. The radio data at different frequencies are displaced relative to one another to avoid overlap. Curves beyond about day 10 are the model predictions that can be tested when more radio data become available (Galama et al., in preparation). Note in particular that the predicted flux decay at 8.46 GHz tends to a relatively shallow power-law of $t^{-1.25}$ (corresponding to $p = 2$ in a wind model; dashed line) before steepening to $t^{-2.2}$ (corresponding to $p = 3.3$). The steepening occurs after day 10^2 , and is not shown.

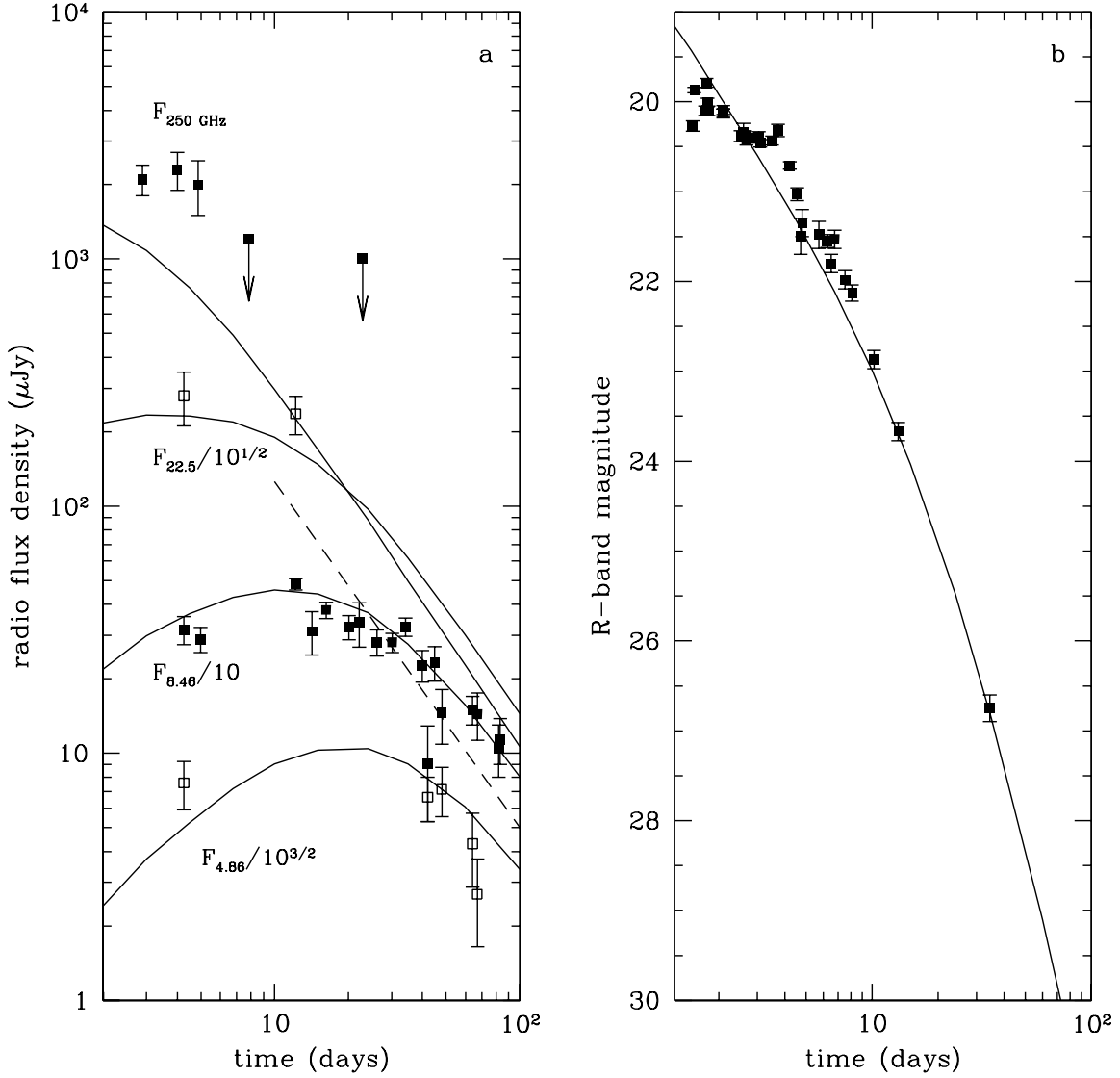


Fig. 2.— Model fits to the observed (a) radio and (b) R-band light curves of GRB 000301C. The radio data at different frequencies are displaced relative to one another to avoid overlap. A power-law of $F_\nu \propto t^{-1.4}$ (corresponding to $p = 2.2$ in a wind model; dashed line) is plotted for reference. The R-band data are increased over the observed values by 15% to account for the Galactic extinction ($E_{B-V} = 0.053$; Schlegel, Finkbeiner & Davis 1998).

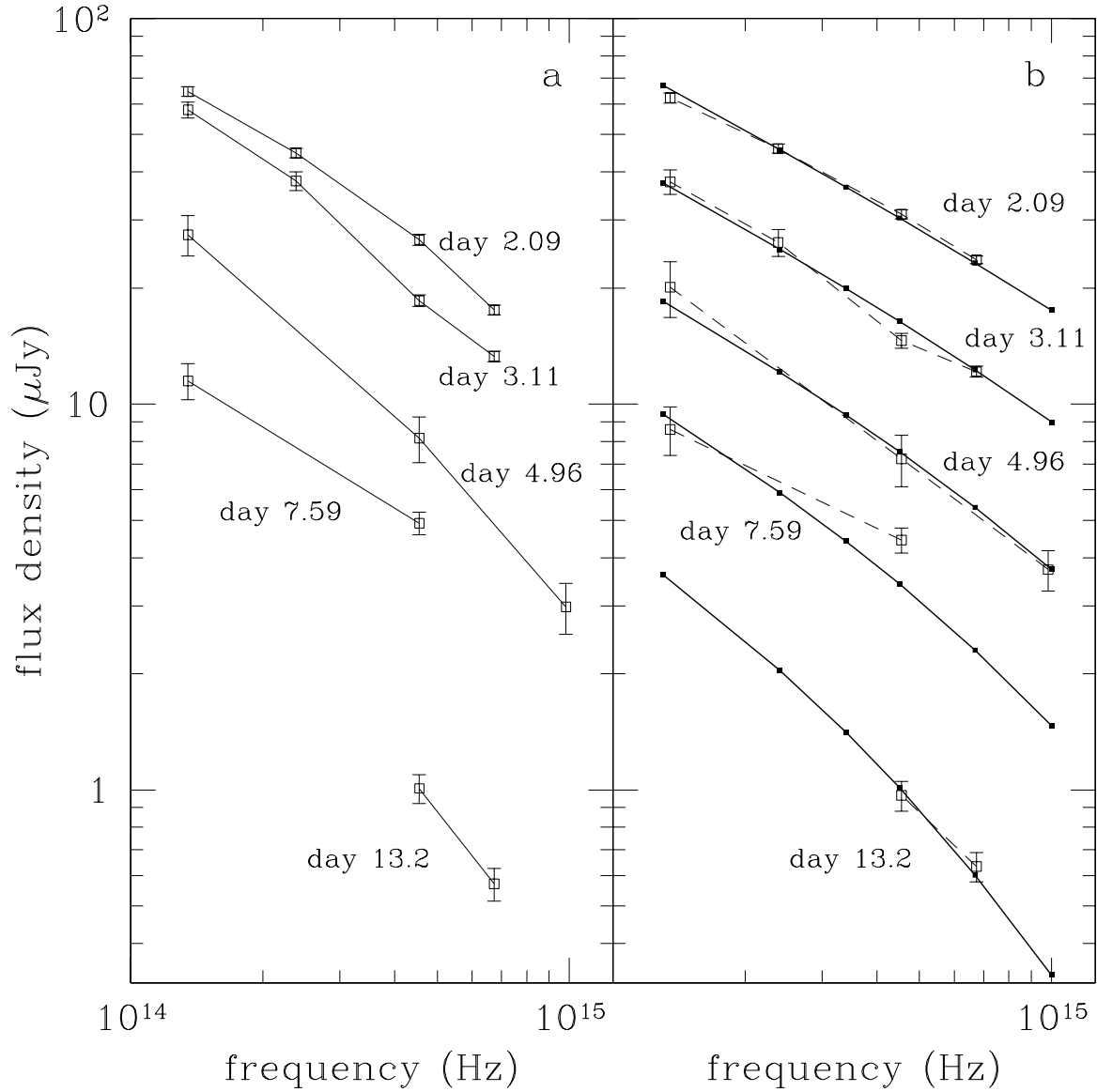


Fig. 3.— The observed (a) and predicted (b) spectral energy distributions of the afterglow of GRB 000301C at several epochs. The observed distributions in (a) are reproduced from Rhoads & Fruchter (2000), with the Galactic extinction already corrected for. The predicted distributions in (b) (solid lines) are generally shallower than their counterparts in (a). A better agreement is achieved when an additional host galaxy extinction of $A_V = 0.09$ of the SMC-type is corrected for (dashed lines; Rhoads & Fruchter 2000). We have adjusted the height of the dashed lines to allow for a better comparison of the slopes of the observed and predicted SEDs.